Chinese Journal of Chemical Engineering 90 (2026) 232–248

Contents lists available at ScienceDirect

Chinese Journal of Chemical Engineering

journal homepage: www.elsevier.com/locate/CJChE

Full Length Article

Sustainability evaluation of novel side-stream extractive distillation incorporating intermediate reboiler process for recovering ethyl acetate and methanol from wastewater based on multi-objective optimization

Ruimin Zhang , Shuang Yang , Jinlong Li *, Hui Wang , Tan Dai , Qing Ye *

Jiangsu Key Laboratory of Advanced Catalytic Materials and Technology, School of Petrochemical Engineering, Changzhou University, Changzhou 213164, China

ARTICLE INFO

Article history:
Received 14 July 2025
Received in revised form
18 September 2025
Accepted 19 September 2025
Available online 30 October 2025

Keywords:
Ternary system with double binary azeotropes
Side-stream extractive distillation
Intermediate reboiler
Multi-objective optimization
Heat integration technology

ABSTRACT

Although side-stream extractive distillation (SED) is widely applied in azeotropic mixture separation due to its high efficiency and energy-saving advantages, the use of expensive high-pressure steam increases economic costs. The introduction of intermediate reboiler (IR) can reduce the consumption of high-pressure steam and thus reduce the operating cost. This work selects the extractive distillation process, using dimethyl sulfoxide (DMSO) as the solvent to separate ethyl acetate and methanol from wastewater. Based on the system characteristics, two SED processes are designed: SED-1 process directly obtains high-purity DMSO from the bottom of the SED column, whereas SED-2 process obtains a DMSO/water mixture at the bottom. To reduce high-pressure steam requirements, an IR is incorporated, leading to the proposal of SED-IR-1 and SED-IR-2 processes. Finally, heat-integrated processes (H-SED-IR-1 and H-SED-IR-2) are proposed based on the optimal SED-IR-1 and SED-IR-2 processes, which utilized the solvent stream waste heat to heat the IR to further reduce the energy consumption and operating cost. The results demonstrate that the H-SED-IR-1 process exhibits optimal economic performance with a 26.19% reduction in total annual cost compared with the conventional extractive distillation (CED) process, while the innovative H-SED-IR-2 process shows outstanding environmental benefits, achieving 38.78% and 39.97% reductions in CO_2 emissions and entropy generation, respectively, compared to the CED process.

1. Introduction

Ethyl acetate (EtOAc) and methanol are two essential compounds with extensive applications in chemical synthesis, pharmaceutical manufacturing, and fine chemical production [1,2]. Industrial processes such as polyvinyl alcohol or aminothiaoxime acid (*i.e.*, aspartate) production and the synthesis of pharmaceutical intermediates like 2-(2-aminothiazol-4-yl)-2-methoxyiminoacetic acid generate significant quantities of EtOAc/methanol mixed waste annually. The direct discharge of these components as wastewater would not only cause significant environmental pollution but also result in substantial resource wastage. Consequently, the development of efficient recycling technologies is both environmentally and economically beneficial and is in line with the core objectives of green chemistry and sustainable development. In recent years, researchers have studied the separation of the EtOAc/methanol/water ternary system [3–6]. Yang *et al.* [7] proposed a triple-column extractive distillation (ED) process with side-reboiler (TCED-SR) for the separation of a high-water content system consisting of 5% (mol) EtOAc, 5% (mol) methanol, and 90% (mol) water, achieving 34% reduction in total annual cost (TAC) and 39% lower CO_2 emissions compared to conventional processes. Alternatively, Zhao *et al.* [8] designed a pressure-swing batch distillation (PSBD) process to treat this ternary system consisting of 48% (mol) EtOAc, 28% (mol) methanol, and 24% (mol) water, achieving 99.9% purity for EtOAc and water. Although PSBD avoids the introduction of solvents, the purity of methanol only reaches 99.5%.

* Corresponding authors.
E-mail addresses: lijinlong@cczu.edu.cn (J. Li), huagonglou508@126.com (Q. Ye).

https://doi.org/10.1016/j.cjche.2025.09.018

Many reports have proved the effectiveness of ED in separating multiple azeotropic systems [9–12]. However, ED is an energy-intensive process, and its energy conservation has attracted much attention with the aim of balancing separation efficiency and energy consumption to provide better solutions for industrial applications [13,14]. The side-stream extractive distillation (SED) process has emerged as a research focus in recent years owing to its significant energy-saving advantages in separation processes [15,16]. In conventional SED process design, solvent recovery is typically achieved by directly obtaining high-purity solvent from the bottom of the side-stream column (SC). Tututi-Avila *et al.* [17] investigated the separation of ethanol/water mixtures using ethylene glycol as the solvent. The results demonstrated that compared to ED process, the SED process reduces energy consumption by 13.5%, TAC by 12.4%, and CO_2 emissions by 13.5%. Wang *et al.* [11] investigated the separation of acetonitrile/benzene/methanol ternary mixtures. The result also demonstrated that the SED process with pure solvent from the bottom of the SC performed best in terms of energy efficiency and economic performance.

However, it should be noted that this approach of obtaining pure solvent from the bottom of the SC often requires maintaining relatively high bottom temperatures. As a result, the SED process often requires significant use of expensive high-pressure steam compared to the ED process, which significantly increases operating costs. Several literatures have reported that the SED process is potentially flawed and does not always save economic costs. Wang *et al.* [18] designed a double SED process for separating chloroform/*n*-hexane/acetone mixtures. Compared to the ED process, although the energy consumption of the double SED process was reduced by 5.1%, its TAC increased by 9.6% owing to the reliance on costly high-pressure steam. Kong *et al.* [19] investigated the separation of ethanol/tetrahydrofuran mixtures in which the corresponding enhancement processes did not provide any energy savings. Compared to the ED process, the SED process not only increases the TAC by 16.5%, but also increases the energy consumption by 6.24%. This is primarily due to the generation of high-purity solvent at the bottom of the SC, which leads to high temperatures at the bottom of the SC. As a result, the bottom reboiler of the SC typically necessitates costly high-pressure steam for heating, potentially leading to an increase in TAC.

To address this limitation, researchers have begun exploring alternative approaches to obtain mixed products from the bottom of the SC, aiming to reduce the bottom temperature. Wang *et al.* [20] investigated five SED processes using ethylene glycol as the solvent to separate the ternary azeotropic system of acetonitrile/isopropanol/water, characterized by the presence of three binary azeotropes. To reduce the bottom temperature of the SC, all five SED processes were designed to obtain mixtures rather than pure solvent at the bottom of the SC. The authors explored the effect of obtaining different composition mixtures from the bottom of the SC on the overall process energy savings. Although the SED process for obtaining mixtures from the bottom of the SC showed limited improvement for the system, it provides novel ideas for developing highly efficient and energy-saving SED process. Liu *et al.* [21] investigated four SED processes for separating the cyclohexanone/acetic acid/water ternary mixture containing two binary azeotropes, using N-methylacetamide (NMA) as the solvent. The difference between the four SED processes is whether high purity NMA or NMA/cyclohexane mixtures are obtained from the bottom of the SC. The results showed that among the four processes, the first SED process which obtained the mixture from the bottom of the SC had the best comprehensive performance. Therefore, the SED process of obtaining the mixture from the bottom of the SC may be a better choice for separating such ternary mixtures. So far, there have been few research literature reports on the SED process for obtaining mixtures at the bottom of the SC.

Furthermore, intermediate reboiling is also an energy-efficient and cost-effective technology widely adopted in distillation processes, which reduces operating costs by partially replacing high-pressure steam with low-pressure steam. Li *et al.* [22] demonstrated that introducing intermediate reboilers (IRs) significantly improved process performance in separating the isopropanol/acetonitrile/water system. The PHI-HI1 scheme with a single IR reduced total costs by 34.9% and energy consumption by 47.9%, while the optimized PHI-HI2 scheme with dual IRs achieved a 36.2% reduction in total costs, 48.5% decrease in energy consumption, and 48.6% reduction in emissions. Xu *et al.* [23] investigated the process of introducing an IR into SED processes to separate the *n*-hexane/EtOAc/acetonitrile ternary mixture. The introduction of IRs in the three SED processes enables partial substitution of high-pressure steam with low-pressure steam, thus reducing the requirment of high-pressure steam in SC. Comparing the process, these modified processes achieve significant reductions in both TAC and energy consumption. Therefore, the integration of IRs effectively lowers operating costs by minimizing high-pressure steam dependency in the bottom reboiler of SC.

In the work, ED and SED processes are employed for the separation of the EtOAc/methanol/water ternary mixture. The EtOAc/methanol/water system exhibits unique separation characteristics by forming two binary azeotropes (EtOAc/methanol and EtOAc/water), where EtOAc can be directly distilled from the top of SC after adding solvent, while the remaining methanol/water mixture (non-azeotropic) can be separated by conventional distillation. Based on this property, two distinct SED processes (SED-1 and SED-2) were developed. The SED-1 process directly obtains high-purity solvent from the bottom of the SC, whereas the SED-2 process produces a solvent/water mixture at the bottom of the SC that requires further separation in a solvent recovery column. To further reduce the operating costs, the SED-1 and SED-2 processes incorporating an IR (SED-IR-1 and SED-IR-2) are developed. A multi-objective optimization targeting TAC, CO_2 emissions, and entropy generation is performed for the five processes, with the optimal solution selected using the TOPSIS method. Furthermore, heat integration technology is introduced into the SED-IR-1 and SED-IR-2 processes to further reduce energy consumption and costs. Ultimately, a comprehensive comparative evaluation of all seven processes is conducted from economic, environmental, and thermodynamic perspectives.

2. Methods

Fig. 1 presents the overall framework for achieving separation of EtOAc/methanol/water mixtures. It consists of four main parts: fundamental research, process design, multi-objective optimization and process evaluation. First, the optimal solvent is selected based on σ-profile hydrogen bond interaction analysis and relative volatility assessment, and the most suitable operating pressure is determined by comparing the relative volatility changes of the system at various pressures. Building upon this, the conventional extractive distillation (CED) process is designed, with optimal operating parameters obtained through multi-objective optimization. Then two different SED (SED-1 and SED-2) processes are proposed according to the unique separation properties of the EtOAc/methanol/water system. To further enhance energy efficiency, an IR is incorporated into the SED-1 and SED-2 processes. Subsequently, corresponding heat integration-assisted processes are designed based on temperature difference analysis between streams. Finally, through a comprehensive evaluation of

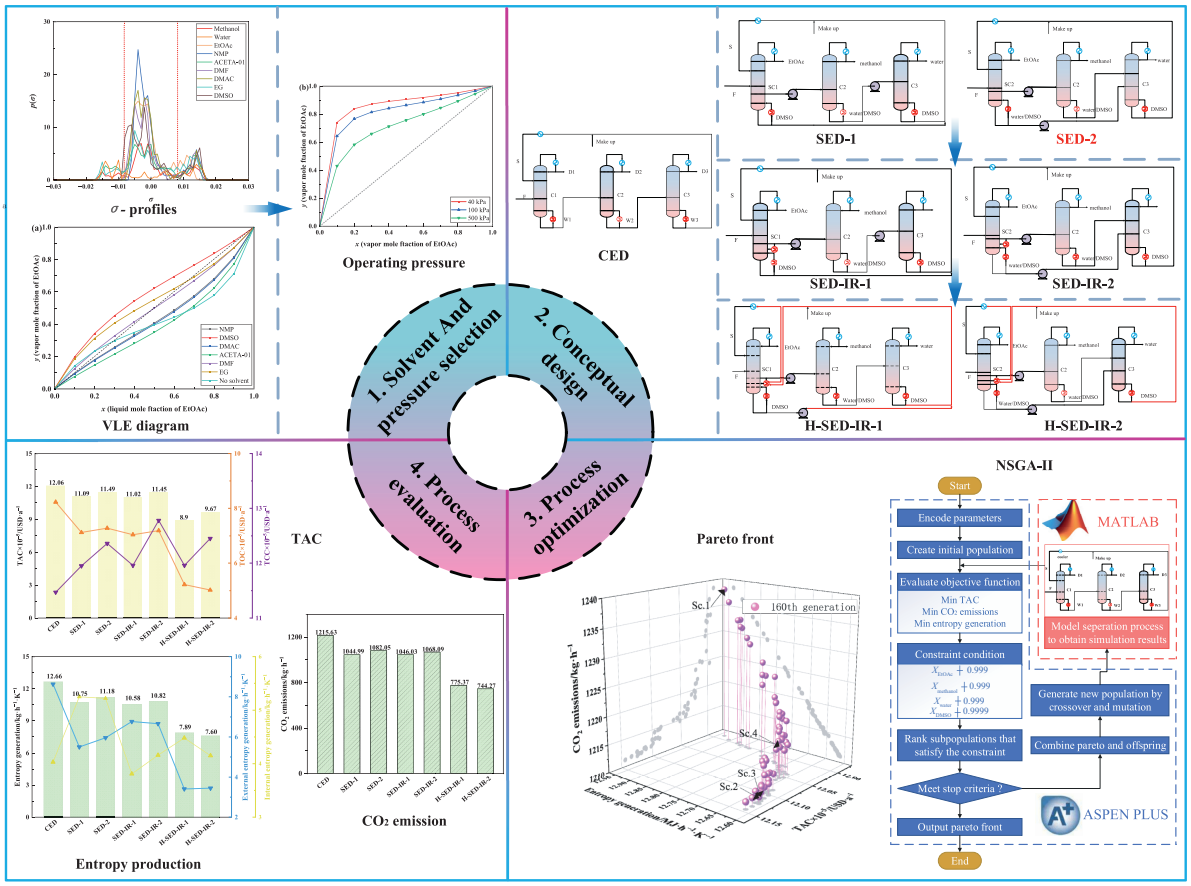

Fig. 1. Schematic illustration of the overall framework.

sustainability indicators, including economic cost, CO_2 emissions, and entropy generation, the optimal process for separating the EtOAc/methanol/water ternary system is determined.

2.1. Thermodynamic method

The EtOAc/methanol/water mixture forms two distinct binary azeotropes at 101.325 kPa: EtOAc/methanol and EtOAc/water. This azeotropic behavior renders conventional distillation ineffective, making ED regarded as an effective separation method for separating this system. In this work, the non-random two-liquid (NRTL) model serves as the thermodynamic method, and simulations are performed for each steady-state process using Aspen Plus (V11). The binary interaction parameters, obtained from the thermodynamic database in Aspen Plus V11, are listed in Table 1. Moreover, as can be seen from Fig. S1 (in Supplementary Material), the predicted data shows good agreement with the experimental data [24–26], which demonstrates the reliability of the NRTL model employed in this study.

2.2. Solvent selection

The effectiveness of ED critically depends on the appropriate selection of solvents, which modify the relative volatilities of system components to disrupt azeotropic behavior. This investigation focuses on the ternary azeotropic system comprising EtOAc, methanol, and water, containing two azeotropes (EtOAc/methanol and EtOAc/water). Initial solvent screening based on polarity considerations identifies *N*-methyl-2-pyrrolidone (NMP), acetamide (ACETA-01), dimethyl sulfoxide (DMSO), ethylene glycol (EG), *N*,*N*-dimethylformamide (DMF), and dimethylacetamide (DMAC) as potential candidates. As shown in Fig. 2, molecular-level interactions are examined through COSMO-SAC computational analysis, which generates surface charge density distributions (σ-profiles) for each solvent system [27]. The obtained σ-profiles clearly demarcate two characteristic interaction domains: the hydrogen bond donating area ($\sigma < -0.82$ e·nm^{-2}) and the hydrogen bond accepting area ($\sigma > 0.82$ e·nm^{-2}). The σ-profiles clearly show pronounced peaks in the hydrogen bond acceptor region for all

Table 1
The binary interaction parameters from the NRTL model.

Component *i*	Component *j*	A_{ij}	A_{ji}	B_{ij}	B_{ji}	C_{ij}
EtOAc	Methanol	0	0	211.7217	173.8828	0.2962
EtOAc	Water	−3.7198	9.4632	1286.1383	−1705.6830	0.2000
EtOAc	DMSO	0	0	287.1115	127.1164	0.3000
Methanol	Water	−0.6930	2.7322	172.9871	−617.2687	0.3000
Methanol	DMSO	0	0	30.5966	−331.1557	0.3000
Water	DMSO	−1.2449	1.7524	586.8010	−1130.2155	0.3000

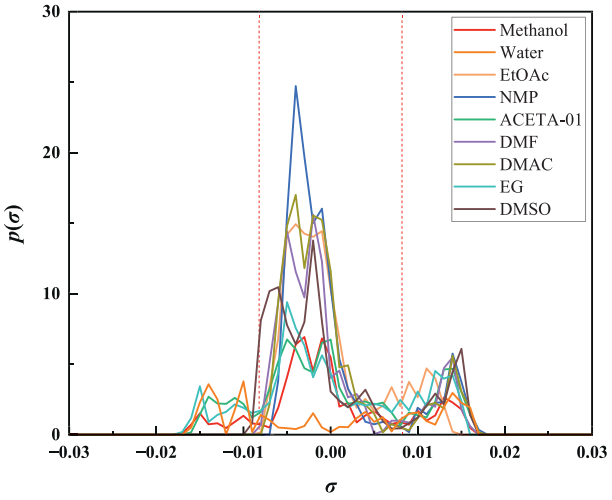

Fig. 2. σ Profiles of EtOAc, methanol, water, and solvents.

candidate solvents, with DMSO exhibiting particularly strong acceptor characteristics. Analysis of σ-profiles for the two azeotropic systems demonstrates that DMSO exhibits strong hydrogen-bond accepting capability with both methanol and water, suggesting this solvent may serve as the optimal solvent for separation of the EtOAc/methanol/water azeotropic mixture.

In ED process, solvents are employed to modify the relative volatilities of components, thereby facilitating their separation. Thus, the effectiveness of various solvents is assessed by relative volatility. The influence of different solvents on the vapor–liquid equilibrium (VLE) of the EtOAc/methanol and EtOAc/water systems is evaluated using Aspen Plus. For this ternary azeotropic system, Fig. 3 presents the VLE curves of the two components when the solvent-to-feed molar ratio is maintained at 1:1. The relative volatility (α) of an azeotrope approaches or equals 1, meaning component separation becomes increasingly favorable as their relative volatility exceeds 1 [28]. The relative volatility is calculated by Eq. (1):

$$\alpha = \frac{y_A/y_B}{x_A/x_B} \tag{1}$$

where x and y stand for the liquid and vapor phase composition, respectively; A and B stand for the volatile and non-volatile components, respectively; α indicates relative volatility.

In VLE diagrams, the diagonal represents $\alpha = 1$. The intersection of no-solvent VLE data with this diagonal confirms azeotrope formation. Thus, the degree of deviation between the VLE curve and the diagonal serves as an indicator of the solvent's separation performance. Comparative analysis reveals that DMSO demonstrates superior performance in enhancing the relative volatilities of both the EtOAc/methanol and EtOAc/water systems. In conclusion, DMSO is determined to be the optimal solvent selection for this separation process. It is found through thermodynamic analysis that this system has unique separation performance. Unlike the typical separation process for ternary azeotropic systems, only one extractive distillation column is required for the process, while the other two are conventional distillation columns. With the addition of the solvent, EtOAc can be preferentially separated as the light component from the top of the extractive distillation column, leaving the methanol/water mixture that can be directly separated by conventional distillation due to its non-azeotropic nature.

2.3. Pressure influence

In the ED process, operating pressure plays a pivotal role in determining separation efficiency. The relative volatility of the components may be highly sensitive to changes in operating pressure, which directly influences the separation efficiency of the process [29]. The EtOAc/methanol and EtOAc/water systems are analyzed using DMSO as the solvent, while the methanol/water system is studied without any solvent addition. Fig. 4 presents the relative volatility behavior of each binary pair in the ternary mixture under different operating pressures. It is evident that changes in operating pressure have a pronounced effect on the relative volatility of the EtOAc/methanol and EtOAc/water systems. As the pressure decreases, the relative volatility of the EtOAc/methanol and EtOAc/water systems increases, which significantly enhances the separation efficiency. To take advantage of low-cost cooling water, the C1 condenser temperature needs to be kept above 50 °C. Therefore, the operating pressure of C1 is ultimately determined to be 40 kPa. In contrast, the relative

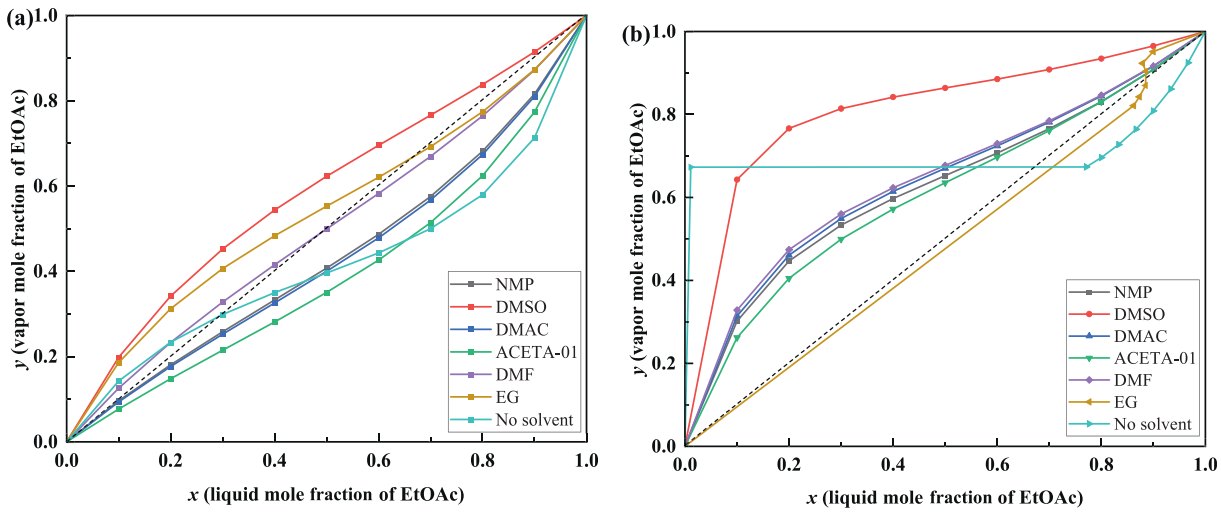

Fig. 3. Effects of solvents on binary azeotropic pairs: (a) EtOAc/methanol; (b) EtOAc/water.

volatility of the methanol/water system exhibits little sensitivity to pressure changes. To reduce operational costs, atmospheric pressure is selected for the separation of this system.

3. Multi-objective Optimization

TAC, entropy generation, and CO_2 emissions, which respectively reflect the economic feasibility, thermodynamic irreversibility, and environmental impact of the separation process, are three key optimization objective functions. However, these optimization objectives are often in conflict with each other, rendering it problematic to obtain the ideal values of all objectives simultaneously. This is a limitation that traditional optimization methods struggle to address effectively. To address this challenge, a multi-objective optimization strategy is implemented using the non-dominated sorting genetic algorithm II (NSGA-II), a well-established method for solving complex optimization problems [30–32]. The distillation process simulation is developed using Aspen Plus V11, followed by multi-objective optimization conducted through MATLAB 2021B. The connection of the two software is established *via* the COM server. The parameters used are shown in Table S1 [33–35]. The specific implementation procedure of the NSGA-II algorithm is schematically illustrated in Fig. 5.

The optimization process generates a set of Pareto-optimal solutions by simultaneously balancing the three objectives, thereby constructing a comprehensive Pareto front. When the values of the variables stabilize during the continuous iteration process, which means that the changes are small, then the optimization is considered to be over [36]. The final optimal solution is selected using an entropy-weighted TOPSIS approach [37,38].

3.1. Economic metric

The economic aspect plays a pivotal role in assessing the viability of distillation processes. In separation processes, the TAC is commonly optimized as the primary objective function. The TAC comprises two main components: the total operating cost (TOC) and the total capital cost (TCC). The relationship between these costs is expressed by Eq. (2).

$$\mathrm{TAC} = \mathrm{TOC} + \frac{\mathrm{TCC}}{\mathrm{PP}} \tag{2}$$

In this analysis, the payback period (PP) is defined as 3 years, requiring the TCC to be divided by 3 for the computation of the TAC [39,40]. The TCC covers the expenses of key equipment, such as distillation columns, heat exchange units (including condensers,

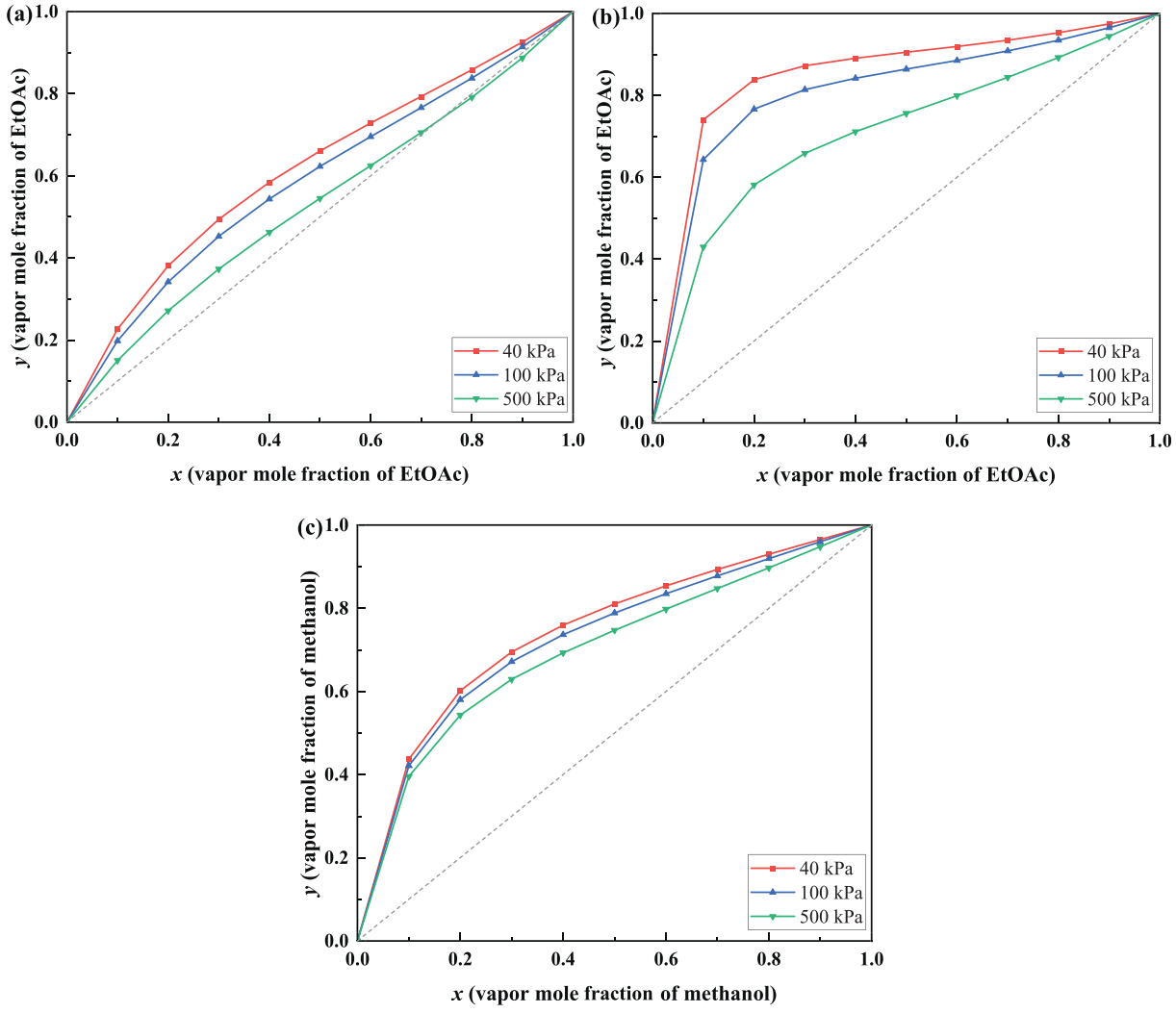

Fig. 4. Effects of pressure on binary azeotropic and non-azeotropic pairs: (a) EtOAc/methanol; (b) EtOAc/water; (c) methanol/water.

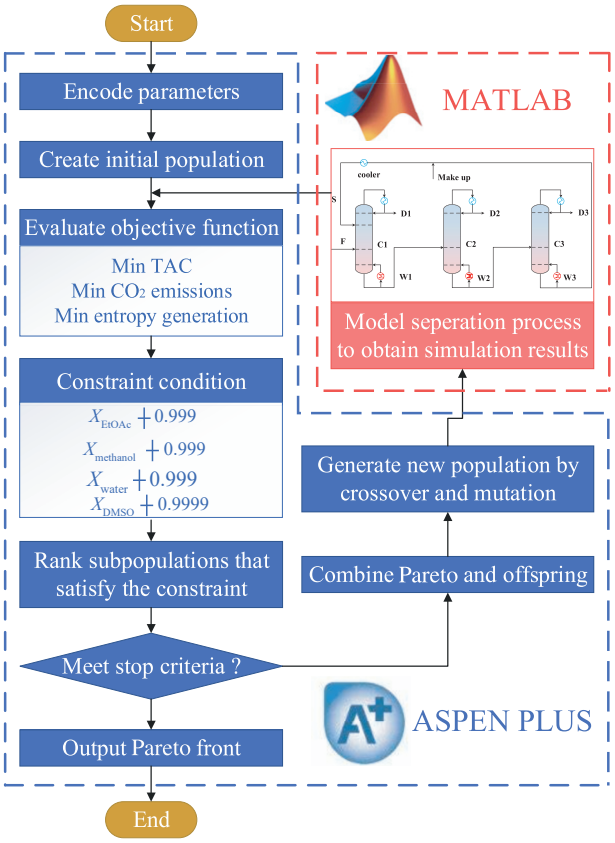

Fig. 5. The specific steps of the NSGA-II algorithm.

reboilers, heaters, and coolers). However, auxiliary components like pipelines, pumps, and valves are excluded from the TCC estimation, as their costs are considered minimal in small-scale operations. Meanwhile, the TOC focuses on utility expenses, such as steam (classified by low, medium, and high pressure), cooling water, and electrical power. Specific calculation methods and utility pricing details are outlined in Table S2.

3.2. Environment metric

In the context of global climate change, CO_2 emissions have become a critical environmental concern [41]. Consequently, CO_2 emissions are adopted as a key metric to assess the environmental impact of the process. Equipment utilizing steam as a heating medium are identified as primary sources of CO_2 emissions. The calculation method of CO_2 emissions is shown in Eqs. (3) and (4) [42].

$$CO_2\ \text{emissions} = \frac{Q_{\text{fuel}}}{\text{NHV}} \times \frac{C}{100}\alpha \tag{3}$$

$$Q_{\text{fuel}} = \left(\frac{Q_{\text{steam}}}{\lambda_{\text{steam}}}\right) \times (h_{\text{steam}} - 419) \times \left(\frac{T_F - T_0}{T_F - T_S}\right) \tag{4}$$

where Q_{fuel} represents the energy released during fuel combustion, C is the CO_2 content (%), NHV is the net calorific value of the fuel, and α is the molar mass ratio of CO_2 to C (3.67) [15]. Additionally, Q_{steam} represents the heat duty of the process, h_{steam} stands for the enthalpy of steam, λ_{steam} stands for the latent heat of steam, and T_S, T_F, and T_0 denote the stack temperature, flame temperature, and ambient temperature, respectively.

3.3. Entropy generation metric

Entropy is a fundamental state function in thermodynamics that characterizes the degree of disorder in a system. According to the second law of thermodynamics, the entropy of an isolated system can never decrease spontaneously. It either remains constant or increases. This implies that any spontaneous process results in an increase in the total entropy generation of the system and its surroundings. Therefore, entropy generation analysis is essential for assessing process irreversibility [35]. This analytical approach serves as a robust thermodynamic tool, enabling the precise identification of energy loss mechanisms and offering valuable insights for process optimization [43]. A higher entropy generation indicates greater irreversibility, while lower entropy generation suggests reduced irreversibility.

To better understand the sources of irreversibility, the total entropy generation is categorized into internal and external generation [44]. External entropy generation primarily includes entropy produced by heat exchange equipment, such as condensers and reboilers, which are integral to the distillation process. Internal entropy generation is the sum of the entropy generated by each plate within the column. The detailed calculation of entropy generation is shown in Eqs. (S1)–(S11) [43,44].

4. Process Design and Optimization

For common ternary azeotropic systems containing two binary azeotropes, an ED process involving two extractive distillation columns is normally required for separation. However, the EtOAc/methanol/water system demonstrates special characteristics. Although it contains two azeotropes (EtOAc/methanol and EtOAc/water), the addition of a solvent allows EtOAc to be directly separated in just one extractive distillation column (C1). The remaining methanol/water mixture, which does not form an azeotrope, can be effectively separated using conventional distillation columns (C2 and C3). This unique property substantially simplifies the process while reducing both capital expenditure and energy requirements.

The molar fractions of EtOAc, methanol, and water in fresh feed are 0.48, 0.28, and 0.24, respectively, and the flow rate of the fresh feed is assumed to be 100 $\text{kmol}\cdot\text{h}^{-1}$ in this investigation [8]. The product purity of EtOAc, methanol, and water are all constrained to 0.999. The purity of DMSO in the circulating solvent stream is specified as 0.9999. The pressure drop for each theoretical stage is set to 274 Pa [45].

4.1. Conventional extractive distillation process

4.1.1. Design of CED process

The CED process consists of one extractive distillation column (C1) and two solvent recovery columns (C2 and C3). The fresh feed and DMSO solvent are introduced into C1 through separate feed plates. High-purity EtOAc is collected as the distillate from C1, while the bottom of the SC containing the methanol/water/DMSO ternary mixture is fed to C2 for subsequent separation. In C2, high-purity methanol is obtained as the distillate, and the residual water/DMSO binary mixture is transferred to C3 for final processing. Ultimately, high-purity water and DMSO are obtained from the top and bottom of C3, respectively. The recovered DMSO is cooled and then recycled back to C1 for reuse, with a small amount of fresh DMSO being supplemented to compensate for solvent losses during the process.

4.1.2. Optimization of the CED process

With the minimum TAC, entropy generation, and CO_2 emissions as objective functions, the NSGA-II is used to optimize the CED process design variables. Meanwhile, the design specifications are incorporated to meet product purity requirements. In the CED process, there are eight design variables to be optimized: the solvent flow rate (S), the solvent feed location (N_S), and the total theoretical plates (N_{P1}, N_{P2}, N_{P3}) along with their respective feed locations (N_{F1}, N_{F2}, N_{F3}) for columns C1, C2, and C3. The Pareto front of the CED process is shown in Fig. 6, demonstrating a range of different optimization scenarios. Detailed parameters are provided in Table S3. Scenarios 1, 2, and 3 (Sc.1, Sc.2, and Sc.3) represent the solutions that minimize the TAC, CO_2 emissions, and entropy generation, respectively. Scenario 4 (Sc.4) is ultimately determined as the best scheme for the CED process, achieving a balanced compromise among process economics, environmental friendliness, and thermodynamic irreversibility through the TOPSIS method.

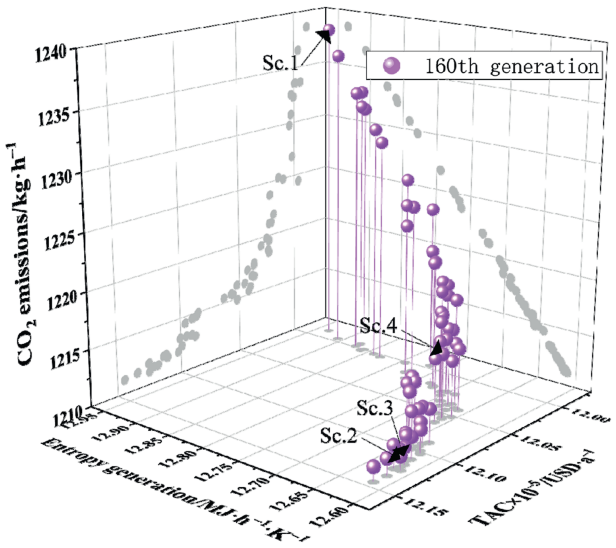

Fig. 6. Pareto front of the CED process.

The optimized CED process and its specific parameters are detailed in Fig. 7. The operating pressures for C1, C2 and C3 are 40, 100 and 100 kPa, respectively. The total theoretical plates N_{P1}, N_{P2}, and N_{P3} are 62, 49, and 24, respectively. The fresh feed enters C1 from the 47th plate and solvent enters C1 from the 4th plate at a flow rate of 144.73 kmol·h^{-1}. The distillate from the top of C1 achieves a purity of 0.999 for EtOAc, while the bottom mixture is directed to the 35th plate of C2. Subsequently, methanol with a purity of 0.999 is distilled from the top of C2, and the mixture at the bottom of C2 is directed to the 8th plate of C3 for further separation. Ultimately, water is distilled from the top of C3, and the solvent DMSO with a purity of 0.9999 is recovered from the bottom. The recovered DMSO is cooled and then recycled back to C1 for reuse, with a small amount of fresh DMSO being supplemented to compensate for solvent losses during the process. The reboiler heat duties for the three columns (C1, C2, and C3) are 1389.40, 931.90, and 758.72 kW, respectively. The optimized CED process achieves TAC of 12.06 × 10^5 USD·a^{-1}, with the TOC and TCC being 8.23 × 10^5 and 11.47 × 10^5 USD·a^{-1}, respectively. The total entropy generation of the CED process is 12.66 MJ·h^{-1}·K^{-1}, with internal and external entropy generation contributing 4.03 and 8.63 MJ·h^{-1}·K^{-1}, respectively. The process emits 1215.63 kg·h^{-1} of CO_2.

Fig. 8 shows the liquid composition distribution in the CED system. The methanol purity reaches a maximum value of 25.87% (mol) at plate 58 of C1, whereas it decreases to only 10.31% (mol) at the C2 feed plate. This significant reduction demonstrates methanol remixing in C1, which leads to increased energy consumption in C2.

4.2. Design and optimization of side-stream extractive distillation process

To mitigate the remixing of methanol, two SED processes are proposed based on the optimal CED process, as shown in Fig. 9. The first side-stream extractive distillation (SED-1) process obtains high-purity DMSO (0.9999) directly as the bottom product of the SED column (SC1).

The second side-stream extractive distillation (SED-2) utilizes the unique separation characteristics of the system to obtain a DMSO/water mixture at the bottom of the SED column (SC2). This mixture then undergoes further separation in a solvent recovery column (C3) to achieve the desired product purity.

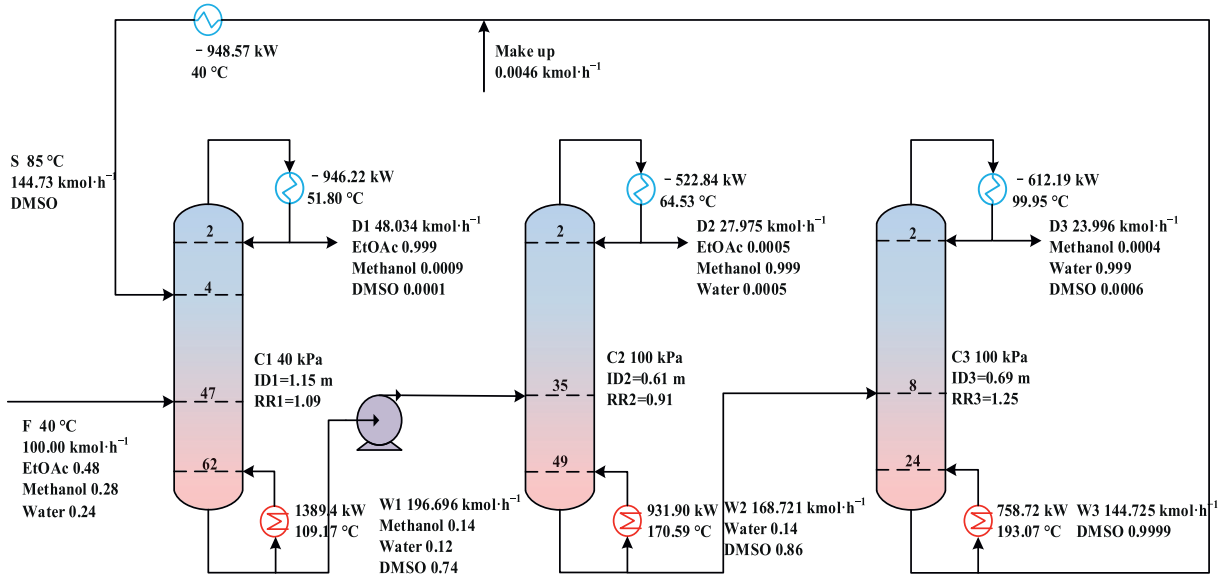

Fig. 7. Process design of CED process for separating EtOAc/methanol/water.

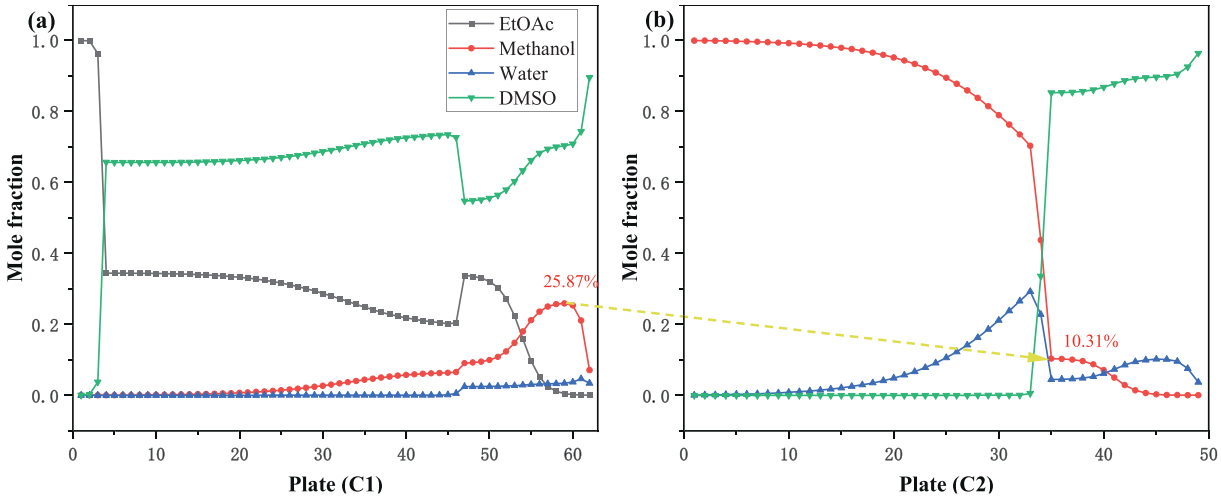

Fig. 8. Liquid composition profiles for CED process: (a) C1 and (b) C2.

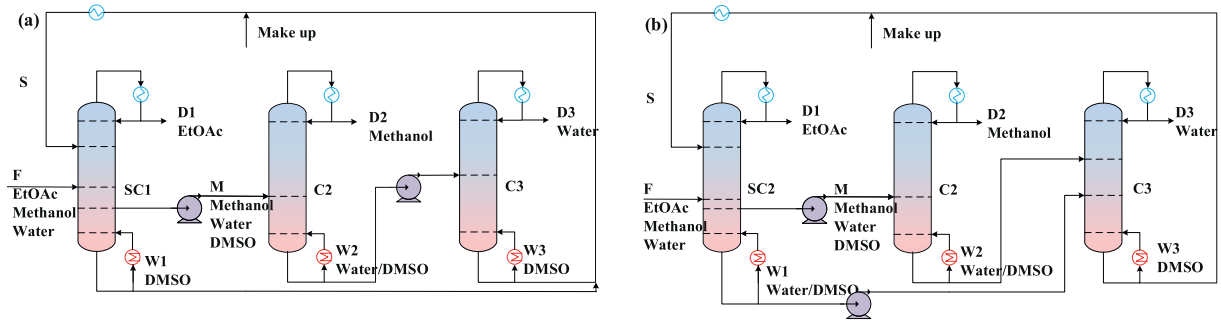

Fig. 9. The conceptual designs of two side-stream extractive distillation processes: (a) SED-1 and (b) SED-2.

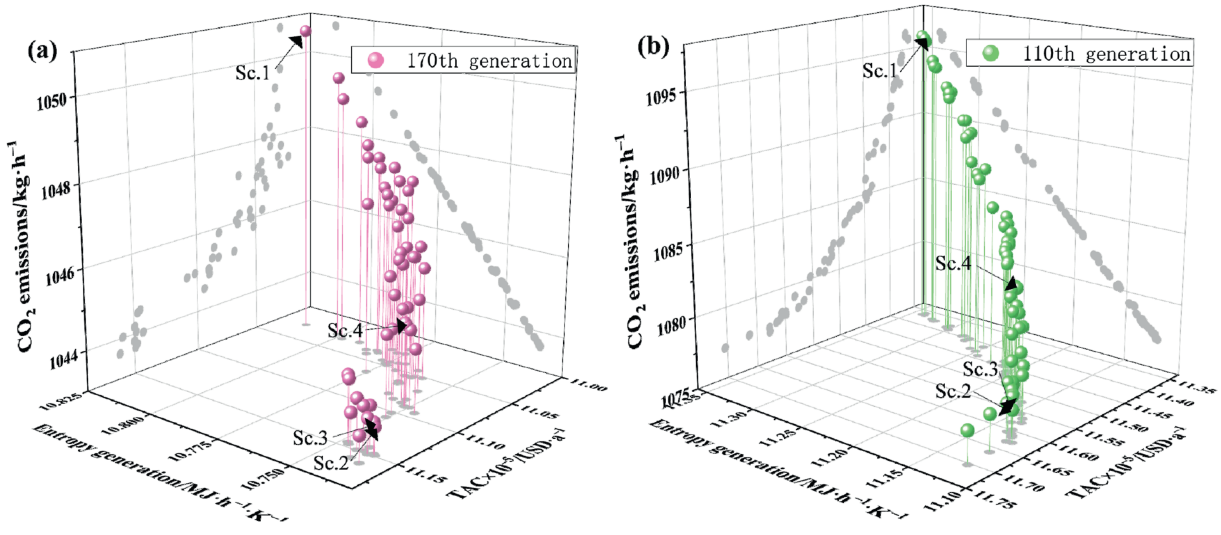

Fig. 10. Pareto front of the (a) SED-1 and (b) SED-2 processes.

The SED-1 and SED-2 processes consist of a SED column (SC1 or SC2), a conventional distillation column (C2), and a solvent recovery column (C3). The products of EtOAc, methanol, and water are distilled from the tops of SC1/SC2, C2, and C3, respectively. Additionally, a side-stream containing a mixture of methanol/water/DMSO is withdrawn from the intermediate plate of SC1/SC2 and fed directly to C2. The intermediate component, methanol, is entirely removed from SC1 by side-stream. The key difference between these two processes is the different components obtained at the bottom of the SC1 and SC2. In the SED-1 process, high-purity DMSO is obtained from the bottom of SC1, while in the SED-2 process, the bottom product is a water/DMSO mixture that needs

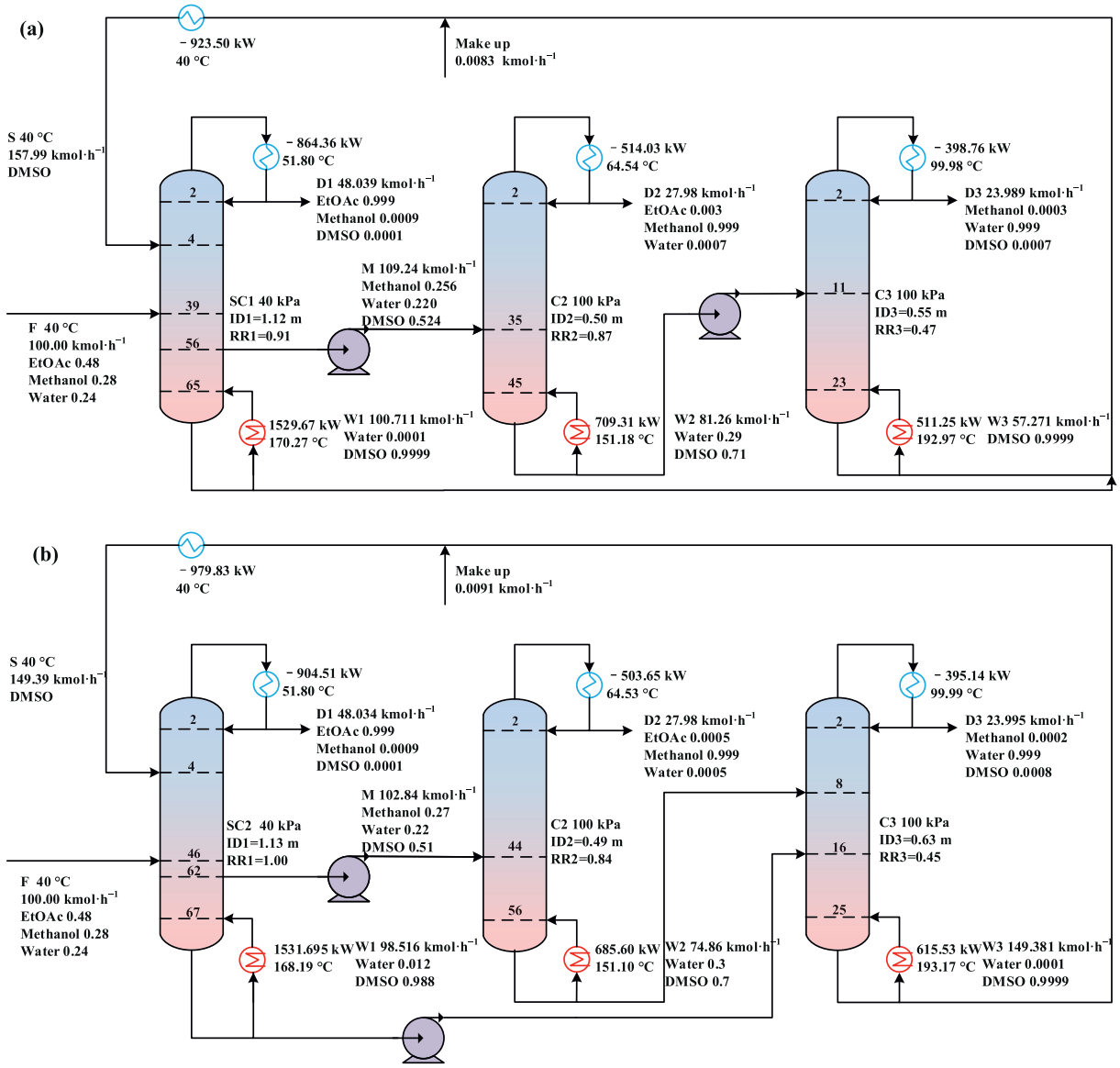

Fig. 11. Process design of (a) SED-1 and (b) SED-2 processes for separating EtOAc/methanol/water.

to be further separated in C3. Finally, the high-purity DMSO stream is cooled and then mixed with the solvent makeup stream before being recycled to SC1/SC2.

In the SED-1 process, there are ten design variables to be optimized: the solvent flow rate (S) and its feed location (N_S), the side-stream flow rate (M) and its withdrawal location (N_M), as well as the total theoretical plates (N_{P1}, N_{P2}, N_{P3}) and feed locations (N_{F1}, N_{F2}, N_{F3}) for columns SC1, C2, and C3. The SED-2 process requires optimization of one additional variable compared to SED-1, as the water/DMSO mixture obtained from the bottom of SC2 needs further separation in C3. Therefore, the optimization variables for the SED-2 process include: the solvent flow rate (S) and its feed location (N_S), the side-stream flow rate (M) and its withdrawal location (N_M), as well as the total theoretical plates (N_{P1}, N_{P2}, N_{P3}) and feed locations (N_{F1}, N_{F2}, $N_{F3\text{-}1}$, $N_{F3\text{-}2}$) for columns SC2, C2, and C3.

The Pareto fronts of SED-1 and SED-2 processes are shown in Fig. 10. They present a range of different optimization scenarios, as detailed in Table S4. Sc.1, Sc.2, and Sc.3 represent the solutions that minimize TAC, CO_2 emissions, and entropy generation, respectively. Sc.4 is the best scheme selected by the TOPSIS method.

The optimized SED-1 and SED-2 processes and its specific parameters are detailed in Fig. 11. The reboiler heat duties for the three columns (SC1, C2, and C3) of the SED-1 process are 1529.67, 709.31, and 511.25 kW, respectively. The optimized SED-1 process achieves TAC of 11.09×10^5 USD·a^{-1}, with the TOC and TCC being 7.03×10^5 and 12.18×10^5 USD·a^{-1}, respectively. The total entropy generation of the SED-1 process is 10.75 MJ·h^{-1}·K^{-1}, with internal and external entropy generation contributing 5.25 and 5.50 MJ·h^{-1}·K^{-1}, respectively. The process emits 1044.99 kg·h^{-1} of CO_2.

The SC2, C2, and C3 of the SED-2 process are 1531.69, 685.60, and 615.53 kW, respectively. The optimized SED-2 process achieves TAC of 11.49×10^5 USD·a^{-1}, with the TOC and TCC being 7.28×10^5 and 12.63×10^5 USD·a^{-1}, respectively. The total entropy generation of the SED-2 process is 11.18 MJ·h^{-1}·K^{-1}, with internal and external entropy generation contributing 5.22 and 5.96 MJ·h^{-1}·K^{-1}, respectively. The process emits 1082.05 kg·h^{-1} of CO_2.

Fig. 12 shows the liquid composition distribution in the SED-1 and SED-2 processes. In the SED-1 process, the purity of methanol reaches its maximum value (22.67% (mol)) at plate 48 of SC1, with 20.48% (mol) maintained at the C2 feed plate. In the SED-2

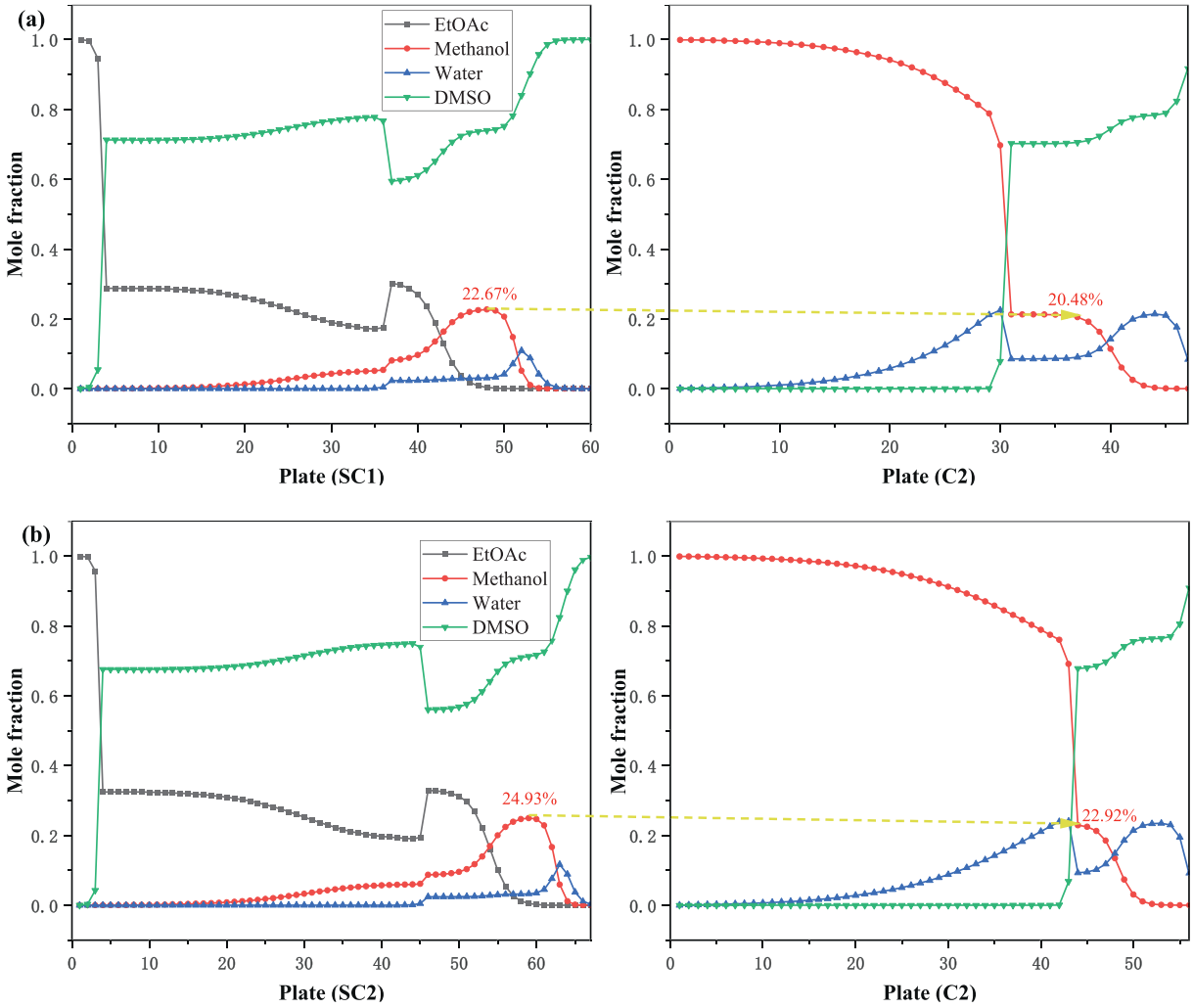

Fig. 12. Liquid composition profiles for (a) SED-1 and (b) SED-2 processes.

process, the purity of methanol reaches its maximum value (24.93% (mol)) at plate 59 of SC2, with 22.92% (mol) maintained at the C2 feed plate. The results show that both the SED-1 and SED-2 processes can effectively eliminate the remixing of methanol.

Compared to the CED process, the SED-1 process achieves reductions of 8.02% in TAC, 14.04% in CO_2 emissions, and 15.08% in entropy generation, while the SED-2 process demonstrates reductions of 4.66% in TAC, 10.99% in CO_2 emissions, and 11.68% in entropy generation. The introduced side-stream alleviates methanol remixing phenomena, resulting in decreased TAC and lower CO_2 emissions. However, the bottom of SC1 and SC2 is heated by relatively expensive medium-pressure steam, resulting in a less energy-saving effect on TAC than on CO_2 emissions.

4.3. Side-stream extractive distillation processes incorporating an intermediate reboiler

To further reduce the medium-pressure steam demand for the reboiler at the bottom of the SC1 and SC2, the SED-1 and SED-2 processes incorporating an IR (SED-IR-1 and SED-IR-2) is proposed, as shown in Fig. 13. Based on the optimized SED-1 and SED-2 process, an IR is installed in each of SC1 and SC2 to partially

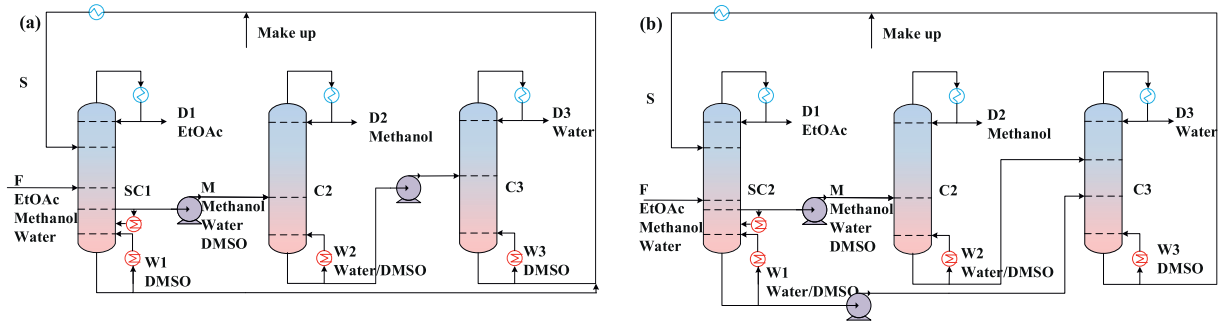

Fig. 13. The conceptual designs of two side-stream extractive distillation processes incorporating an IR: (a) SED-IR-1 and (b) SED-IR-2.

replace the medium-pressure steam requirement with low-pressure steam. Subsequently, NSGA-II is employed to optimize the process. Compared with the SED-1 and SED-2 processes, the SED-IR-1 and SED-IR-2 processes have two additional optimization variables: the vapor fraction (V_f) and liquid stream flow rate (F_L) of the IR.

The Pareto fronts of SED-IR-1 and SED-IR-2 processes are shown in Fig. 14. They present a range of different optimization scenarios, as detailed in Table S5. Sc.1, Sc.2, and Sc.3 represent the solutions that minimize TAC, CO_2 emissions, and entropy generation, respectively. Sc.4 is the best scheme selected by the TOPSIS method.

The optimized SED-IR-1 and SED-IR-2 processes and its specific parameters are detailed in Fig. 15. The SC1, C2, and C3 of the SED-IR-1 are 773.38, 721.08, and 521.32 kW, respectively. The optimized SED-IR-1 process achieves TAC of 11.02 × 10^5 USD·a^{-1}, with the TOC and TCC being 7.04 × 10^5 and 11.96 × 10^5 USD·a^{-1}, respectively. The total entropy generation of the SED-IR-1 process is 10.58 MJ·h^{-1}·K^{-1}, with internal and external entropy generation contributing 3.81 and 6.77 MJ·h^{-1}·K^{-1}, respectively. The process emits 1046.03 kg·h^{-1} of CO_2.

The SC2, C2, and C3 of the SED-IR-2 are 606.67, 694.31, and 614.58 kW, respectively. The optimized SED-IR-2 process achieves TAC of 11.45 × 10^5 USD·a^{-1}, with the TOC and TCC being 7.19 × 10^5 and 12.78 × 10^5 USD·a^{-1}, respectively. The total entropy generation of the SED-IR-2 process is 10.82 MJ·h^{-1}·K^{-1}, with internal and external entropy generation contributing 4.16 and 6.66 MJ·h^{-1}·K^{-1}, respectively. The process emits 1068.09 kg·h^{-1} of CO_2.

Fig. 16 illustrates the temperature profiles in SC1 and SC2 for SED-IR-1 and SED-IR-2 processes. In SC1, The heat duties of the bottom reboiler and the IR are 773.38 and 775.04 kW respectively. Since the high purity solvent with a temperature of 169.94 °C is obtained from the bottom of SC1, the bottom reboiler must be heated using medium-pressure steam. Whereas, the IR can be heated with cheaper low-pressure steam due to the lower temperature of the plate. In SC2, with bottom reboiler and the IR requirements measuring 606.67 kW and 926.75 kW respectively. The 168.68 °C solvent product from the bottom of SC2 similarly mandates medium-pressure steam for the bottom reboiler, while the IR can be heated with low-pressure steam. The implementation of this approach in SED-IR-1 and SED-IR-2 processes demonstrates significant potential for operational cost reduction through optimized energy utilization.

Fig. 17 shows the liquid composition distribution in the SED-IR-1 and SED-IR-2 processes. In the SED-IR-1 process, the purity of methanol reaches its maximum value (22.37% (mol)) at plate 48 of SC1, with 20.82% (mol) maintained at the C2 feed plate. In the SED-IR-2 process, the purity of methanol reaches its maximum value (25.45% (mol)) at plate 60 of SC2, with 22.09% (mol) maintained at the C2 feed plate. The results show that the SED-IR-1 and SED-IR-2 processes are not only able to reduce the TAC but also well eliminate the remixing of methanol.

Compared to the CED process, the SED-IR-1 process achieves reductions of 8.58% in TAC, 13.95% in CO_2 emissions, and 16.47% in entropy generation, while the SED-IR-2 process demonstrates reductions of 5.03% in TAC, 12.14% in CO_2 emissions, and 14.57% in entropy generation. Since the IR of the SED-IR-1 and SED-IR-2 processes is heated with low-pressure steam, TAC and CO_2 emissions are further decreased compared to the SED-1 and SED-2 processes.

4.4. Heat-integrated side-stream extractive distillation processes incorporating an intermediate reboiler

The IR requires low-pressure steam heating, while the high-temperature solvent flow obtained at the bottom of column will cause a large amount of heat waste when cooled. To optimize energy utilization, we develop two heat-integrated SED processes (H-SED-IR-1 and H-SED-IR-2) that effectively recover and utilize this waste heat for the IR heating.

Fig. 18 presents the H-SED-IR-1 process with specific parameters, while Fig. S2 details its heat exchange network (HEN) illustrating the detail heat exchange situations. In the H-SED-IR-1 process, the heat released when the high-purity solvent stream is cooled from 192.77°C to 40 °C, can be used for heating the IR of SC1. A heat input of 775 kW is provided by the solvent stream to the IR of SC1. Consequently, the solvent stream temperature is reduced to 66.6 °C, with a corresponding temperature increase of the liquid stream in the IR from 86.0°C to 142.3 °C. The SC1, C2, and C3 are 773.51, 721.15, and 521.34 kW, respectively. The H-SED-IR-1 process achieves TAC of 8.90 × 10^5 USD·a^{-1}, with the TOC and TCC being 5.22 × 10^5 and 11.96 × 10^5 USD·a^{-1}, respectively. The total entropy generation of the H-SED-IR-1 process is 7.89 MJ·h^{-1}·K^{-1}, with internal and external entropy generation contributing 4.48 and 3.41 MJ·h^{-1}·K^{-1}, respectively. The process emits 775.37 kg·h^{-1} of CO_2. In comparison to the

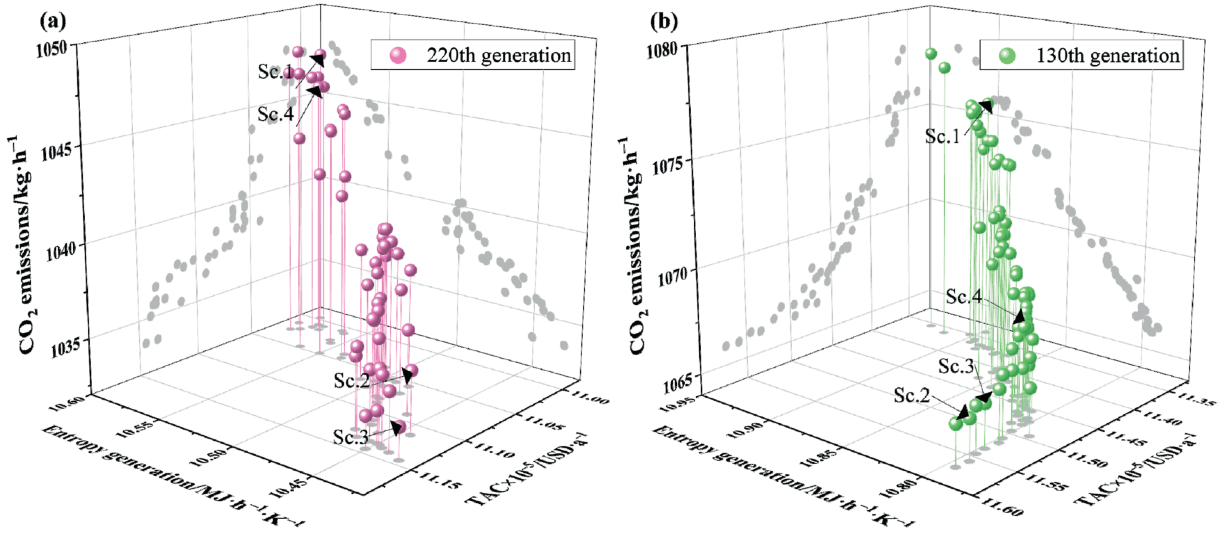

Fig. 14. Pareto front of the (a) SED-IR-1 and (b) SED-IR-2 processes.

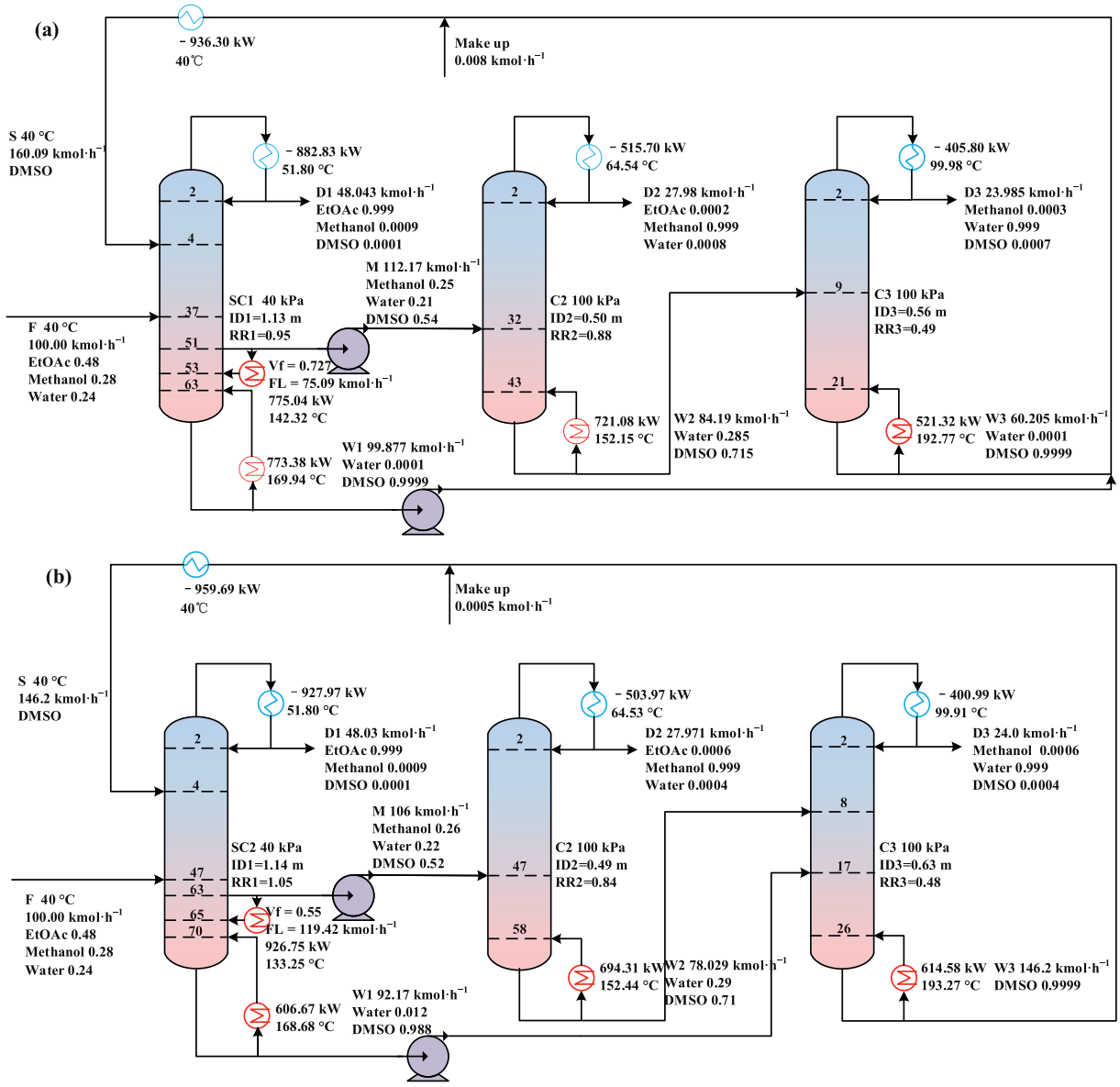

Fig. 15. Process design of (a) SED-IR-1 and (b) SED-IR-2 processes for separating EtOAc/methanol/water.

CED process, the H-SED-IR-1 process achieves reductions of 26.19% in TAC, 36.22% in CO_2 emissions, and 37.68% in entropy generation.

Fig. 19 presents the H-SED-IR-2 process with specific parameters, while Fig. S3 details its HEN illustrating the detail heat exchange situations. In the H-SED-IR-2 process, the heat released when the high-purity solvent stream is cooled from 193.27°C to 40 °C can be used for heating the IR of SC2. A heat input of 926.8 kW is provided by the solvent stream to the IR of SC2. Consequently, the solvent stream temperature is reduced to 46.0 °C, with a corresponding temperature increase of the liquid stream in the IR from 85.8°C to 133.3 °C. The SC2, C2, and C3 are 606.67, 694.31, and 614.58 kW, respectively. The H-SED-IR-2 process achieves TAC of 9.17×10^5 USD·a^{-1}, with the TOC and TCC being 5.02×10^5 and 12.45×10^5 USD·a^{-1}, respectively. The total entropy generation of the H-SED-IR-2 process is 7.60 MJ·h^{-1}·K^{-1}, with internal and external entropy generation contributing 4.15 and 3.45 MJ·h^{-1}·K^{-1}, respectively. The process emits 744.27 kg·h^{-1} of CO_2. In comparison to the CED process, the H-SED-IR-2 process achieves reductions of 23.97% in TAC, 38.78% in CO_2 emissions, and 39.97% in entropy generation.

5. Results and Discussion

5.1. Economic evaluation

Fig. 20 presents a comparative analysis of TOC, TCC, and TAC across seven processes. The results show that due to reduced methanol remixing, the SED-1 and SED-2 processes significantly decrease TOC compared to the CED process, leading to lower TAC. Similarly, the SED-IR-1 and SED-IR-2 processes also reduce TOC, mainly because they can use low-pressure steam in the IR reducing the use of more expensive medium-pressure steam in the bottom reboiler. However, they exhibit increased TCC, attributable to the additional equipment requirements of the IR. Compared to the CED process, the TAC of SED-IR-1 and SED-IR-2 processes is reduced by 8.58% and 5.03% respectively. Furthermore, thermal integration design can be implemented for the SED-IR-1

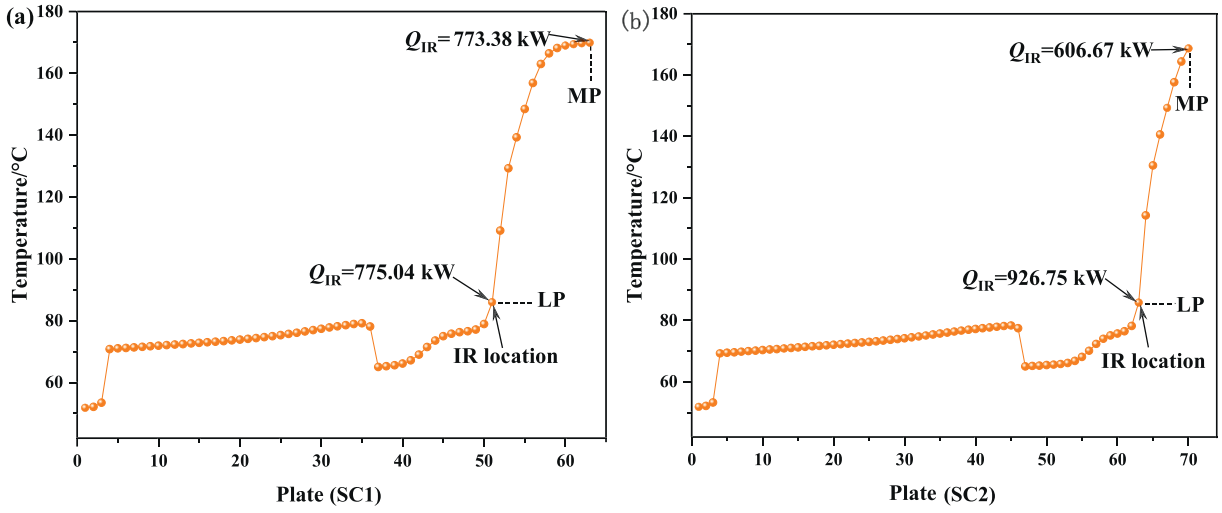

Fig. 16. Temperature profiles of SC1 and SC2 in the (a) SED-IR-1 and (b) SED-IR-2 processes.

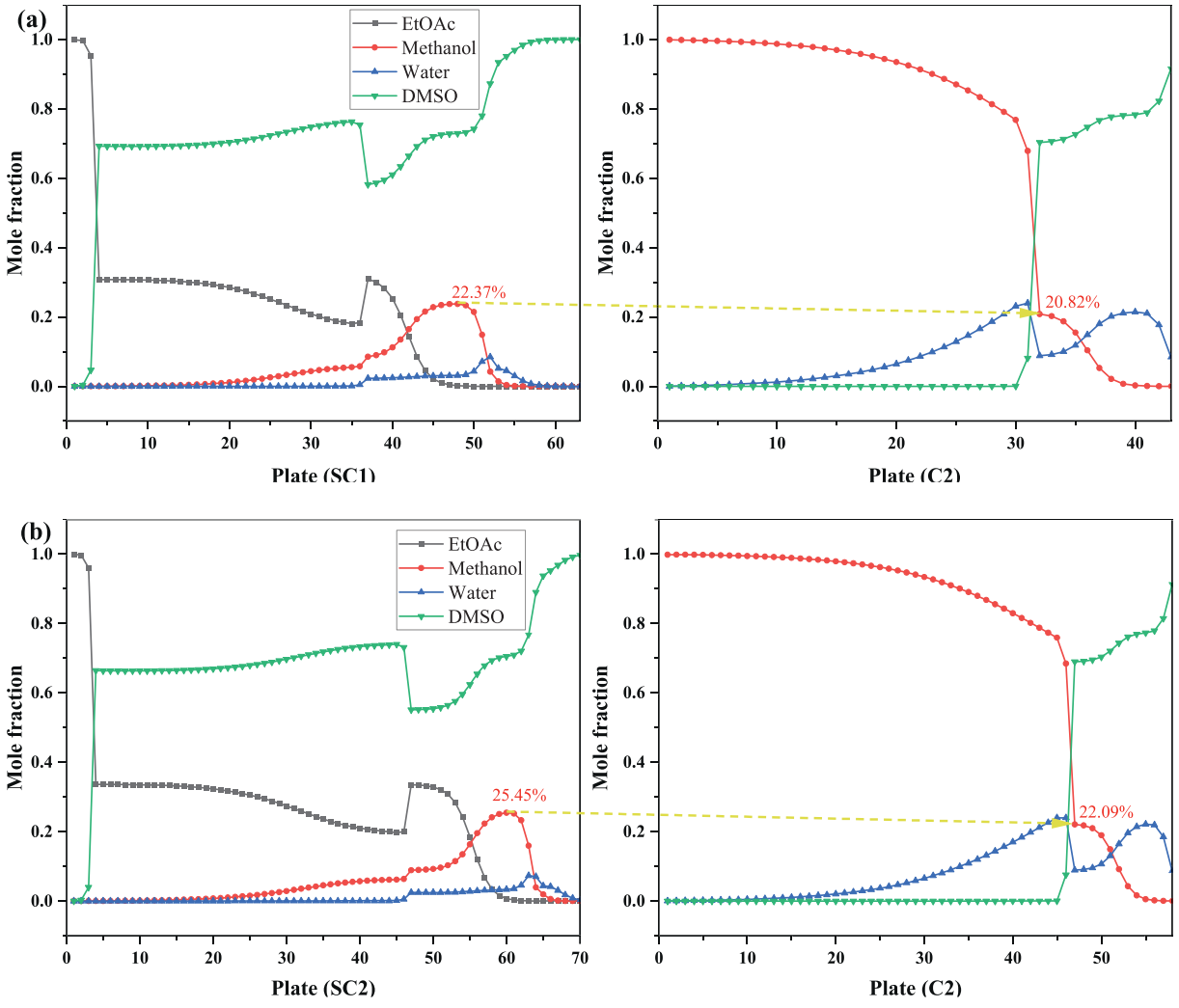

Fig. 17. Liquid composition profiles for (a) SED-IR-1 and (b) SED-IR-2 processes.

and SED-IR-2 processes based on the IR to further reduce TAC. The TAC of H-SED-IR-1 and H-SED-IR-2 processes shows reductions of 26.19% and 23.97% relative to the CED process. Although the H-SED-IR-1 process incurs higher operating costs due to its higher energy consumption compared to the H-SED-IR-2 process, it requires fewer total stages, which results in lower capital costs. Therefore, the H-SED-IR-1 process exhibits the best economic performance.

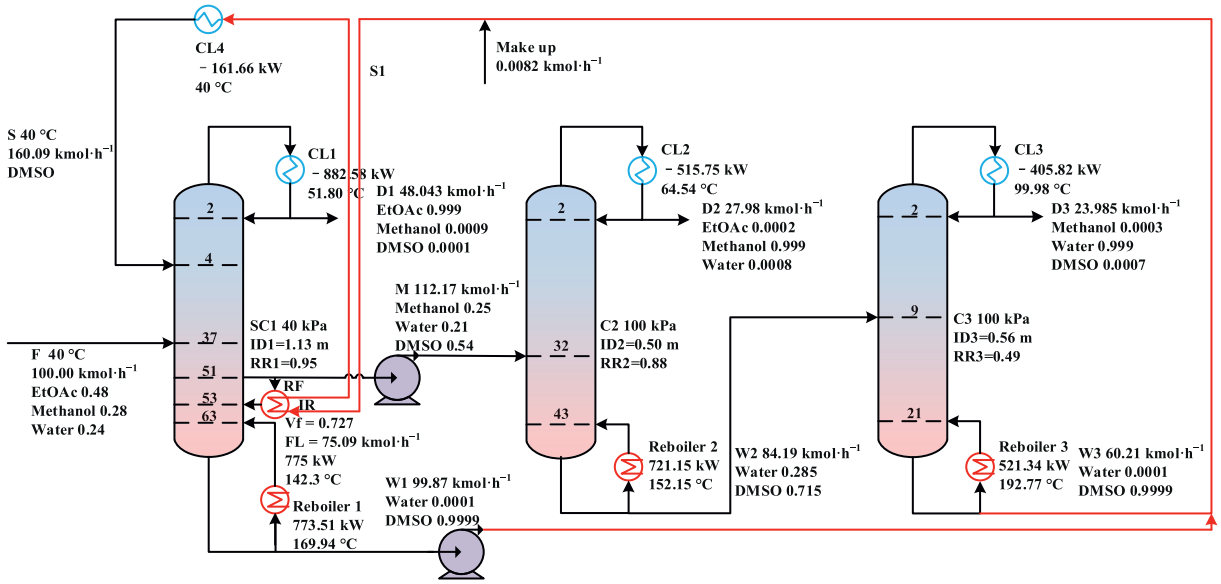

Fig. 18. Process design of H-SED-IR-1 process for separating EtOAc/methanol/water.

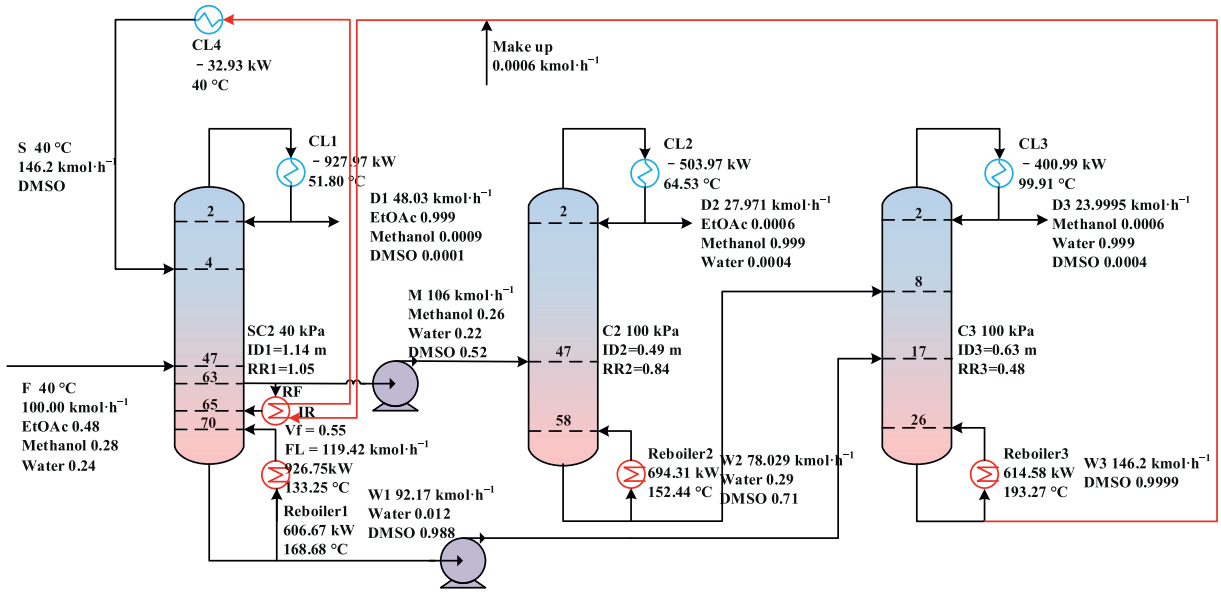

Fig. 19. Process design of H-SED-IR-2 process for separating EtOAc/methanol/water.

5.2. Environment evaluation

Fig. 21 presents a comparative analysis of CO_2 emissions across seven processes. Compared with the CED process, the SED-1 and SED-2 processes reduce CO_2 emissions by 14.04% and 10.99%, respectively. This reduction is due to the fact that C2 in the SED-1 and SED-2 processes is heated by medium-pressure steam, which produces significantly lower CO_2 emissions compared to high-pressure steam, resulting in lower CO_2 emissions for the entire process. In addition, the use of an IR, which is heated by low-pressure steam rather than relying exclusively on medium-pressure steam in the bottom reboiler, again results in a slight reduction in CO_2 emissions. Finally, the adoption of heat integration technology on the basis of the IR can save a large amount of steam consumption and significantly reduce CO_2 emissions. Compared with the CED process, the CO_2 emissions of the H-SED-IR-1 and H-SED-IR-2 processes are reduced by 36.22% and 38.78%, respectively.

Due to the design of the H-SED-IR-2 process that produces a DMSO/water mixture at the bottom of the column, the remixing of components is more effectively suppressed.

Consequently, after heat integration, the H-SED-IR-2 process exhibits lower total energy consumption, which in turn leads to reduced CO_2 emissions. In summary, the H-SED-IR-2 process outperforms the other processes in emission reduction performance.

5.3. Entropy generation evaluation

Fig. 22 presents a comparative analysis of internal, external, and total entropy generation across seven processes. The internal

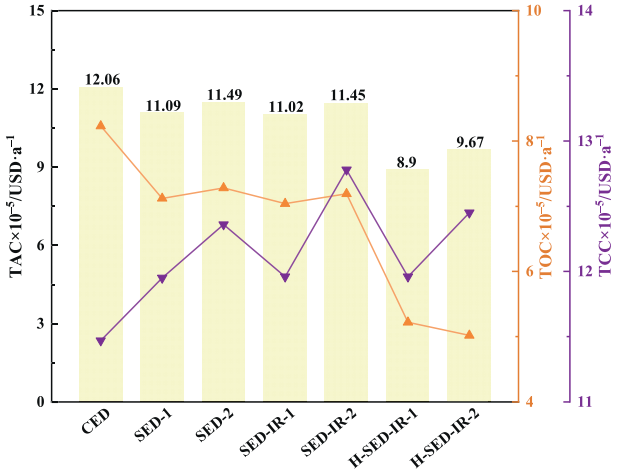

Fig. 20. Economic comparison for TAC, TCC and TOC of the proposed processes.

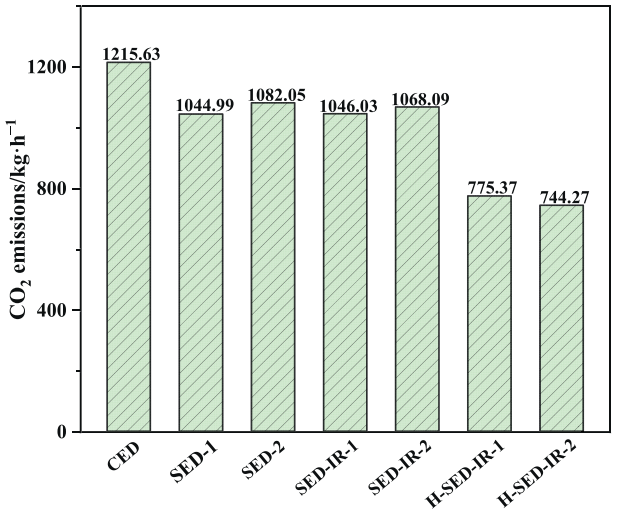

Fig. 21. CO_2 emissions of the proposed processes.

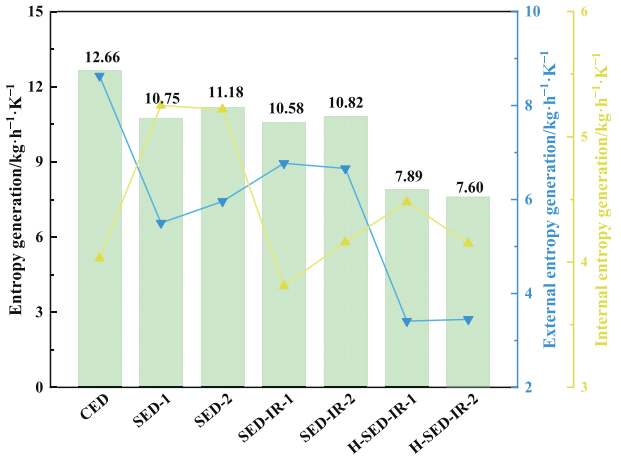

Fig. 22. Entropy generation of the proposed processes.

entropy generation of both the SED-1 and SED-2 processes is higher than that of the CED process. This is due to the fact that the introduction of side-stream increases the irreversibility of the process, resulting in particularly high entropy generation in SC1 and SC2, thereby elevating the overall internal entropy generation of the processes. The reduction in external entropy generation stems from the decreased total energy consumption in the reboiler. Compared with the CED process, the total entropy generation of the SED-1 and SED-2 processes is reduced by 15.08% and 11.68%, respectively. In addition, the incorporation of IRs in SC1 and SC2 allows the use of low-pressure steam for heating, thus reducing the use of medium-pressure steam in the bottom reboiler. Therefore, the use of IR improves the energy efficiency and reduces the entropy generation of the process accordingly. Finally, the introduction of heat integration technology applied to the IR further reduces its energy consumption, resulting in a significant reduction in process entropy generation. Compared with the CED process, the H-SED-IR-1 and H-SED-IR-2 processes reduce the entropy generation by 37.68% and 39.97%, respectively. From the thermodynamic irreversibility point of view, the H-SED-IR-2 process achieves minimal process irreversibility and optimal thermodynamic efficiency among all evaluated systems.

6. Conclusions

In this study, using DMSO as the solvent, two SED processes integrated with IRs were designed for the recovery of EtOAc and methanol from wastewater. In the SED-IR-1 process, high-purity DMSO is obtained from the bottom of SC1, whereas the SED-IR-2 process obtains a DMSO/water mixture from the bottom of SC2. Using TAC, CO_2 emissions, and entropy generation as optimization objectives, the processes are optimized with the NSGA-II algorithm, and heat integration is further incorporated to reduce energy consumption and TAC. The results indicate that the H-SED-IR-1 process exhibits the best economic performance, with a 26.19% reduction in TAC compared to the CED process. The H-SED-IR-2 process demonstrates superior environmental and thermodynamic performance, achieving reductions of 38.78% in CO_2 emissions and 39.97% in entropy generation relative to the CED process. Although the process that produces a mixture at the bottom does not demonstrate significant advantages in this system, it offers valuable insights for the design and optimization of related processes.

Future research will focus on developing dynamic control strategies to enhance the robustness of the process against feed fluctuations, improve its adaptability in complex operating environments, and promote the advancement of distillation technology.

CRediT Authorship Contribution Statement

Ruimin Zhang: Writing – review & editing, Writing – original draft, Methodology, Investigation, Data curation. Shuang Yang: Resources. Jinlong Li: Investigation. Hui Wang: Validation. Tan Dai: Validation. Qing Ye: Writing – review & editing, Supervision, Methodology, Conceptualization.

Declaration of Competing Interest

The authors declare that they do not have any commercial or associative interest that represents a conflict in connection with the work reported in this paper.

Acknowledgements

This work was supported by the National Natural Science Foundation of China (22178030, 21878025, 22078026).

Supplementary Material

Supplementary data to this article can be found online at https://doi.org/10.1016/j.cjche.2025.09.018.

References

[1] C. Wang, Y. Zhuang, Y.T. Qin, Y.C. Dong, L.L. Liu, L. Zhang, J. Du, Optimization and eco-efficiency analysis of extractive distillation processes with different solvents for separating the ternary mixture embedding two azeotropes, *Sep. Purif. Technol.* 269 (2021) 118763.

[2] X.H. Li, Q. Ye, J.L. Li, L.Q. Yan, X. Jian, L.C. Xie, J.Y. Zhang, Investigation of energy-efficient heat pump assisted heterogeneous azeotropic distillation for separating of acetonitrile/ethyl acetate/*n*-hexane mixture, *Chin. J. Chem. Eng.* 55 (2023) 20−33.

[3] J.X. Zhu, A. Yang, H. Zhang, W.F. Shen, Pressure-swing heterogeneous azeotropic distillation for energy-efficient recovery of ethyl acetate and methanol from wastewater with expanded feed composition range, *Comput. Chem. Eng.* 194 (2025) 108956.

[4] A. Yang, S.R. Sun, Z.Y. Kong, S.S. Zhu, J. Sunarso, W.F. Shen, Energy-efficient heterogeneous triple-column azeotropic distillation process for recovery of ethyl acetate and methanol from wastewater, *Comput. Chem. Eng.* 183 (2024) 108618.

[5] A. Yang, Z.Y. Kong, S.R. Sun, J. Sunarso, J.Z. Ren, W.F. Shen, Design and multiobjective optimization of a novel double extractive dividing wall column with a side reboiler scheme for the recovery of ethyl acetate and methanol from wastewater, *Ind. Eng. Chem. Res.* 62 (44) (2023) 18591−18602.

[6] P. Srivastava, A. Gupta, N. Kaistha, Synthesis and integrated design of a compact azeotropic process for EtAc−MeOH−water separation, *Ind. Eng. Chem. Res.* 63 (49) (2024) 21466−21478.

[7] A. Yang, L. Ernawati, M. Wang, Z.Y. Kong, J. Sunarso, S.R. Sun, W.F. Shen, Multi-objective optimization of the intensified extractive distillation with side-reboiler for the recovery of ethyl acetate and methanol from wastewater, *Sep. Purif. Technol.* 310 (2023) 123131.

[8] F. Zhao, Z.F. Xu, J.G. Zhao, J. Wang, M.Y. Hu, X. Li, Z.Y. Zhu, P.Z. Cui, Y.L. Wang, Y.X. Ma, Process design and multi-objective optimization for separation of ternary mixtures with double azeotropes *via* integrated quasi-continuous pressure-swing batch distillation, *Sep. Purif. Technol.* 276 (2021) 119288.

[9] J.L. Gu, X.Q. You, C.Y. Tao, J. Li, V. Gerbaud, Energy-saving reduced-pressure extractive distillation with heat integration for separating the biazeotropic ternary mixture tetrahydrofuran−methanol−water, *Ind. Eng. Chem. Res.* 57 (40) (2018) 13498−13510.

[10] T. Shi, A. Yang, S.M. Jin, W.F. Shen, S.A. Wei, J.Z. Ren, Comparative optimal design and control of two alternative approaches for separating heterogeneous mixtures isopropyl alcohol−isopropyl acetate−water with four azeotropes, *Sep. Purif. Technol.* 225 (2019) 1−17.

[11] C. Wang, C. Guang, Y. Cui, C. Wang, Z.S. Zhang, Compared novel thermally coupled extractive distillation sequences for separating multi-azeotropic mixture of acetonitrile/benzene/methanol, *Chem. Eng. Res. Des.* 136 (2018) 513−528.

[12] J. Zhai, Q.B. Sun, C.B. Hao, X.F. Leng, Y.R. Zhou, C.H. Liu, J.Z. Li, Y.K. Wu, Process design, multi-objective optimisation and energy-saving strategies of extractive distillation for separating ternary mixture containing two azeotropes, *Chem. Eng. Sci.* 319 (2026) 122303.

[13] Z.Y. Kong, E. Sánchez-Ramírez, A. Yang, W.F. Shen, J.G. Segovia-Hernández, J. Sunarso, Process intensification from conventional to advanced distillations: past, present, and future, *Chem. Eng. Res. Des.* 188 (2022) 378−392.

[14] Y.K. Zong, H.Y. Lee, J. Sunarso, The evolution of process design and control for ternary azeotropic separation: recent advances in distillation and future directions, *Sep. Purif. Technol.* 284 (2022) 120292.

[15] S.R. Sun, L. Fu, A. Yang, W.F. Shen, An intensified energy-saving architecture for side-stream extractive distillation of four-azeotrope mixtures considering economic, environmental and safety criteria simultaneously, *Sep. Purif. Technol.* 310 (2023) 123132.

[16] A. Yang, Z.Y. Kong, J. Sunarso, Design and optimisation of novel hybrid side-stream reactive−extractive distillation for recovery of isopropyl alcohol and ethyl acetate from wastewater, *Chem. Eng. J.* 451 (2023) 138563.

[17] S. Tututi-Avila, N. Medina-Herrera, J. Hahn, A. Jiménez-Gutiérrez, Design of an energy-efficient side-stream extractive distillation system, *Comput. Chem. Eng.* 102 (2017) 17−25.

[18] C. Wang, Y. Zhuang, Y.C. Dong, C.C. Zhou, L. Zhang, J. Du, Conceptual design of the triple-column extractive distillation processes with single entrainer and double entrainer for separating the *N*-hexane/acetone/chloroform ternary multi-azeotropic mixture, *Chem. Eng. Sci.* 237 (2021) 116578.

[19] Z.Y. Kong, J.G. Segovia-Hernández, H.Y. Lee, J. Sunarso, Are process-intensified extractive distillation always energetically more efficient? *Chem. Eng. Process. Process Intensif.* 181 (2022) 109131.

[20] C. Wang, T.C. Sun, W.A. Chen, Z.T. Tan, Y. Zhuang, J. Du, J. Zhao, Applicability exploration and sustainable assessment of heat integration and vapor recompression heat pump to side-stream extractive distillation processes for separating ternary azeotropic system, *Sep. Purif. Technol.* 345 (2024) 127251.

[21] J.Y. Liu, X.L. Liu, J. Li, J.Y. Ren, J. Wang, L.Y. Sun, Design and control of side-stream extractive distillation to separate acetic acid and cyclohexanone from wastewater by varying pressure, *Process. Saf. Environ. Prot.* 159 (2022) 1127−1149.

[22] Y.D. Li, Q. Ye, N.G. Wang, L.J. Chen, H.X. Zhang, Y.G. Xu, Energy-efficient extractive distillation combined with heat-integrated and intermediate reboilers for separating acetonitrile/isopropanol/water mixture, *Sep. Purif. Technol.* 262 (2021) 118343.

[23] Z.X. Xu, Y. Ding, Q. Ye, J.L. Li, H.B. Wu, J. Pan, Novel energy-efficient design of side-stream extractive distillation process with intermediate reboiler for separating multi-azeotropic mixture based on multi-objective optimization, *Chem. Eng. Sci.* 295 (2024) 120138.

[24] I. Nagata, T. Yamada, S. Nakagawa, Excess Gibbs free energies and heats of mixing for binary systems ethyl acetate with methanol, ethanol, 1-propanol, and 2-propanol, *J. Chem. Eng. Data* 20 (3) (1975) 271−275.

[25] S.E. Kharin, V.M. Perelygin, A.G. Volkov, Liquid−vapor phase equilibrium in ethanol−ethyl acetate and water−ethyl acetate systems, *Izv. Vyssh. Uchebn. Zaved. Pishch. Tekhnol.* (4) (1968) 136−139.

[26] K. Kojima, K. Tochigi, H. Seki, K. Watase, Determination of vapor−liquid equilibrium from boiling point curve, *Chem. Eng* 32 (2) (1968) 149−153, a1.

[27] Y. Xu, D.P. Meng, H.Y. Li, X.P. Yu, Z.Y. Zhu, Y.L. Wang, Y.X. Ma, J. Gao, Mechanism analysis for separation of cyclohexane and *tert*-butanol system *via* ionic liquids as extractants and process optimization, *ACS Sustainable Chem. Eng.* 7 (24) (2019) 19984−19992.

[28] P.Z. Cui, F. Zhao, D. Yao, Z.Y. Ma, S.H. Li, X. Li, L. Wang, Z.Y. Zhu, Y.L. Wang, Y. X. Ma, D.M. Xu, Energy-saving exploration of mixed solvent extractive distillation combined with thermal coupling or heat pump technology for the separation of an azeotrope containing low-carbon alcohol, *Ind. Eng. Chem. Res.* 59 (29) (2020) 13204−13219.

[29] J. Abildskov, J.P. O'Connell, Responses of azeotropes and relative volatilities to pressure variations, *Chem. Eng. Res. Des.* 99 (2015) 97−110.

[30] H.Y. Cheng, Y.Y. Wang, W.X. Wang, C.H. Wen, X.W. Wei, Y. Wang, Y.L. Wang, P.Z. Cui, Z.Y. Zhu, Economic, environmental, exergy (3E) analysis and multi-objective genetic algorithm optimization of efficient and energy-saving separation of diethoxymethane/toluene/ethanol by extractive distillation with mixed extractants, *Energy* 284 (2023) 129262.

[31] Y.Y. Jiao, M. Yan, X.L. Wang, J.H. Zhong, Y.S. Chen, W.G. Zhu, X. Li, Z.Y. Zhu, P. Z. Cui, Y.Y. Lu, Y.L. Wang, Economic, environmental, energy and exergy analysis and multi-objective optimization for efficient purification of a friendly gasoline additive by extractive distillation coupled with pervaporation, *Fuel* 335 (2023) 127069.

[32] K.C. Wang, L.L. Xin, Y. Zhang, J.G. Qi, Z.Y. Zhu, Y.L. Wang, L.M. Zhong, P.Z. Cui, Sustainable and efficient process design for wastewater recovery of cyclohexane/isopropyl alcohol azeotrope by extractive distillation based on multi-objective genetic algorithm optimization, *Chem. Eng. Res. Des.* 201 (2024) 593−602.

[33] Y. Wang, Q. Ye, J.L. Li, Q.Q. Rui, A.Z. Yu, Economic and entropy production evaluation of extractive distillation and solvent-assisted pressure-swing distillation by multi-objective optimization, *Chin. J. Chem. Eng.* 63 (2023) 246−259.

[34] H.R. Zhang, S. Wang, J.X. Tang, N.N. Li, Y.N. Li, P.Z. Cui, Y.L. Wang, S.Q. Zheng, Z.Y. Zhu, Y.X. Ma, Multi-objective optimization and control strategy for extractive distillation with dividing-wall column/pervaporation for separation of ternary azeotropes based on mechanism analysis, *Energy* 229 (2021) 120774.

[35] Q.Q. Rui, Y. Ding, Q. Ye, J.L. Li, Y. Wang, A.Z. Yu, Insights on the sustainable design of extractive distillation processes for separating the isopropanol/1,4-dioxane/water mixture considering economic and entropy generation indicators, *Chem. Eng. Process. Process Intensif.* 193 (2023) 109561.

[36] H. Alcocer-García, J.G. Segovia-Hernández, O.A. Prado-Rubio, E. Sánchez-Ramírez, J.J. Quiroz-Ramírez, Multi-objective optimization of intensified processes for the purification of levulinic acid involving economic and environmental objectives, *Chem. Eng. Process. Process Intensif.* 136 (2019) 123−137.

[37] Z.Y. Luo, S. Yang, N. Xie, W.W. Xie, J.X. Liu, Y.S. Agbodjan, Z.Q. Liu, Multi-objective capacity optimization of a distributed energy system considering economy, environment and energy, *Energy Convers. Manag.* 200 (2019) 112081.

[38] S.R. Pandit, A.K. Jana, Transforming conventional distillation sequence to dividing wall column: minimizing cost, energy usage and environmental impact through genetic algorithm, *Sep. Purif. Technol.* 297 (2022) 121437.

[39] W.C. Shen, I.L. Chien, Design and control of ethanol/benzene separation by energy-saving extraction−distillation process using glycerol as an effective heavy solvent, *Ind. Eng. Chem. Res.* 58 (31) (2019) 14295−14311.

[40] X.Q. You, J.L. Gu, C.J. Peng, I. Rodriguez-Donis, H.L. Liu, Optimal design of extractive distillation for acetic acid dehydration with *N*-methyl acetamide, *Chem. Eng. Process. Process Intensif.* 120 (2017) 301−316.

[41] H.M. Han, Z. Zeeshan, B.A. Talpur, T. Sadiq, U.A. Bhatti, E.M. Awwad, M. Al-Razgan, Y.Y. Ghadi, Studying long term relationship between carbon emissions, soil, and climate change: insights from a global earth modeling framework, *Int. J. Appl. Earth Obs. Geoinf.* 130 (2024) 103902.

[42] M. Gadalla, Ž. Olujić, A. de Rijke, P.J. Jansens, Reducing CO_2 emissions of internally heat-integrated distillation columns for separation of close boiling mixtures, *Energy* 31 (13) (2006) 2409–2417.
[43] H. Benyounes, W.F. Shen, V. Gerbaud, Entropy flow and energy efficiency analysis of extractive distillation with a heavy entrainer, *Ind. Eng. Chem. Res.* 53 (12) (2014) 4778–4791.
[44] R.T. Gooty, J.A. Chavez Velasco, R. Agrawal, Methods to assess numerous distillation schemes for binary mixtures, *Chem. Eng. Res. Des.* 172 (2021) 1–20.
[45] W.L. Luyben, Methanol/trimethoxysilane azeotrope separation using pressure-swing distillation, *Ind. Eng. Chem. Res.* 53 (13) (2014) 5590–5597.